scientific reports

Check for updates

OPEN

Bergenin protects against osteoarthritis by inhibiting STAT3, NF-κB and Jun pathways and suppressing osteoclastogenesis

Zhiwei Zhang[1,2,3,5], Bo Li[1,2,3,5], Shuqin Wu[4,5], Yuxin Yang[4], Binkang Wu[1,2,3], Qi Lai[1,2,3], Fuchong Lai[1,2,3], Fengbo Mo[1,2,3], Yufei Zhong[4], Song Wang[1,2,3]✉, Runsheng Guo[1,2,3]✉ & Bin Zhang[1,2,3]✉

Osteoarthritis (OA) is a chronic degenerative disease characterized by articular cartilage destruction and subchondral bone reconstruction in the early stages. Bergenin (Ber) is a cytoprotective polyphenol found in many medicinal plants. It has been proven to have anti-inflammatory, antioxidant, and other biological activities, which may reveal its potential role in the treatment of OA. This study aimed to determine the potential efficacy of Ber in treating OA and explore the possible underlying mechanism through network pharmacology and validation experiments. The potential co-targets and processes of Ber and OA were predicted by using network pharmacology, including a Venn diagram for intersection targets, a protein−protein interaction (PPI) network to obtain key potential targets, and GO and KEGG pathway enrichment to reveal the probable mechanism of action of Ber on OA. Subsequently, validation experiments were carried out to investigate the effects and mechanisms of Ber in treating OA in vitro and vivo. Ber suppressed IL-1β-induced chondrocyte apoptosis and extracellular matrix catabolism by inhibiting the STAT3, NF-κB and Jun signalling pathway in vitro. Furthermore, Ber suppressed the expression of osteoclast marker genes and RANKL-induced osteoclastogenesis. Ber alleviated the progression of OA in DMM-induced OA mice model. These results demonstrated the protective efficacy and potential mechanisms of Ber against OA, which suggested that Ber could be adopted as a potential therapeutic agent for treating OA.

Keywords Osteoarthritis, Bergenin, Osteoclastogenesis, STAT3, NF-κB, Jun

Abbreviations

OA	Osteoarthritis
Ber	Bergenin
PPI	Protein−protein interaction
NSAIDs	Nonsteroidal anti-inflammatory drugs
ECM	Extracellular matrix
COL2a1	Type II collagen
MMPs	Matrix metalloproteinases
ADAMTSs	A disintegrin and metalloproteinase with thrombospondin motifs protein
INOS	Nitric oxide synthase 2
COX2	Cyclooxygenase 2
NF-κB	Nuclear factor-kappa B
BMMs	Bone marrow macrophages

[1]Department of Orthopedic Hospital, The 1st Affiliated Hospital, Jiangxi Medical College, Nanchang University, No. 17, Yongwaizheng Street, Nanchang 330006, Jiangxi, China. [2]Department of Sports Medicine of Orthopedic Hospital, The 1st Affiliated Hospital, Jiangxi Medical College, Nanchang University, No. 17, Yongwaizheng Street, Nanchang 330006, Jiangxi, China. [3]Artificial Joints Engineering and Technology Research Center of Jiangxi Province, No. 17, Yongwaizheng Street, Nanchang 330006, Jiangxi, China. [4]Faculty of Jiangxi Medical College, Donghu District, Nanchang University, No.461 Bayi Road, Nanchang 330006, Jiangxi, China. [5]These authors contributed equally: Zhiwei Zhang, Bo Li and Shuqin Wu. ✉email: ndyfy10323@ncu.edu.cn; ndyfy02752@ncu.edu.cn; ndyfy01354@ncu.edu.cn

IL-1β	Interleukin-1 beta
M-CSF	Macrophage colony-stimulating factor
RANKL	Receptor activator of nuclear factor kappa-B ligand
ERS	ER stress

Osteoarthritis (OA) is a common degenerative joint disorder characterized by cartilage degeneration, subchondral bone sclerosis, and the formation of osteophytes[1,2]. The typical clinical manifestation of OA is joint pain, accompanied by joint dysfunction, limited mobility, and other symptoms, which greatly reduce the quality of life of patients and cause great economic and medical burdens to society[3]. According to statistics, more than 300 million people suffer from OA symptoms, and the incidence rate has increased rapidly with the increasing prevalence of obesity and the aging population[4,5]. However, the number of FDA-approved OA treatments remains limited, with nonsteroidal anti-inflammatory drugs (NSAIDs) and joint replacements being the current treatments[6]. NSAIDs are accompanied by a large number of side effects, and the life of joint replacement prostheses is still a problem. Therefore, it is particularly important to explore the mechanism of osteoarthritis and explore new strategies for the treatment of OA.

Currently, with the increasing understanding of OA pathology, the prominent feature of OA is considered to be the degradation of articular cartilage, low-grade inflammation, and subchondral bone remodelling[7]. During OA progression, the extracellular matrix (ECM) of articular cartilage, which is composed of aggrecan and type II collagen (COL2a1), is degraded by proteolytic enzymes, including disintegrin and metalloproteinase with thrombospondin motifs (ADAMTSs) and matrix metalloproteinases (MMPs)[8]. Stromal cell-derived factor (SDF)-1 activates the expression of c-Fos and c-Jun, leading to the activation of MMP-13 promoter[9] and prostaglandin E2 (PGE2) inhibits c-Jun to decrease expression levels of MMP-1 and MMP-13[10], indicating that Jun signalling pathway plays an essential role in upregulate the expression of MMP family, promoting the progression of OA. In addition, inflammatory cytokines such as IL-1β are considered to be the most important compounds in the pathogenesis of OA, inducing catabolism of the cartilage matrix[11]. Under inflammatory conditions, chondrocytes not only secrete a series of inflammatory factors, such as inducible nitric oxide synthase 2 (INOS) and cyclooxygenase 2 (COX2) but also activate the nuclear factor-kappa B (NF-κB) and STAT3 signalling pathways in chondrocytes[12]. The NF-κB and STAT3 signalling pathways are classic inflammatory pathways in OA and are related to cartilage degeneration and subchondral bone remodelling in OA[13]. Changes in bone properties, including bone resorption and bone formation, occur after bone injury[14]. Osteoclasts may be affected by proinflammatory cytokines secreted by OA chondrocytes, such as IL-1β, which indirectly induces osteoclast formation and directly induces osteoclast precursors to form multinucleated osteoclasts and release hydrogen ions and catalase for osteolysis, further playing an important role in the pathogenesis of early-stage OA[15]. Currently, increasing research has shown that maintaining a balance between chondrocytes and osteoblasts is crucial because it improves the progression of OA and ameliorates OA-related pain[16,17]. Therefore, therapeutic strategies targeting chondrocytes and osteoblasts may offer new therapeutic approaches for treating OA.

Bergenin (Ber) is a glycoside derivative of trihydroxybenzoic acid extracted from the rhizome of the medicinal plant Bergenia crassifolia. Current studies have shown that it has antioxidant and anti-inflammatory pharmacological effects[18]. Furthermore, Ber and its derivatives were investigated play a role in down-regulating the expression of NF-kB and IKK-β in THP-1 cells, holding the promise of being antiarthritic drugs[19]. Ber prodrugs—Acetyl ester 4a2, also can be potential therapy against rheumatoid arthritis[20].Studies showed that Ber and its natural derivatives are not significantly cytotoxic and do not produce harmful side effects, which demonstrates the potential for clinical applications of Ber[21]. However, whether it can be applied to OA is still unknown. Therefore, we aimed to predict the potential mechanisms of action of Ber in OA through network pharmacological analysis and further validated the predicted mechanisms through experiments, which will ultimately provide new and better therapies for OA patients.

Materials and methods

Preparation of compounds

Ber was solubilized in dimethyl sulfoxide to achieve a 10 mM concentration and subsequently stored at – 80 °C for preservation. This compound was sourced from MedChemExpress (New Jersey, USA).

Network pharmacological analysis

We obtained the molecular structure of Ber from PubChem. The potential binding protein targets of Ber were then identified using PharmMapper and BATMAN-TCM online tools. Moreover, we used the DisGENET database (http://www.disgenet.org), GeneCards database (http://www.genecards.org), DrugBank (https://go.drugbank.com), TTD database (http://db.idrblab.net/ttd/) and PharmGKB (https://www.pharmgkb.org/) to retrieve target genes related to OA. Subsequently, we employed the R language to obtain the main osteoarthritis-related targets potentially targeted by Ber and visualized the protein interactions (PPIs) using Cytoscape software. Key functions and pathways were identified by KEGG and GO analyses, and the main mechanisms by which Ber acts on OA were analysed by Metoscape.

Molecular docking

We removed the ligands, solvent molecules, etc., of the predicted target proteins via Chimera software. At the same time, we extracted the drug structure from PubChem (https://pubchem.ncbi.nlm.nih.gov/) and preprocessed the structure of Ber following the same steps as those described above. Subsequently, we calculated the center and size of Gasteiger and docking stations using AutoDock Tools. Finally, we used AutoDock Vina to perform molecular docking and calculate the binding affinity. The results were displayed by Chimera software.

Cell viability assay

Chondrocyte viability was meticulously evaluated utilizing the Cell Counting Kit-8 (CCK-8) assay in strict accordance with the manufacturer's comprehensive guidelines. Initially, chondrocytes were seeded onto 96-well plates at a density of 70,000 cells per cm2 and allowed to adhere for 24 h. Subsequently, the chondrocytes were treated with varying concentrations of Ber (0, 2.5, 5, 10, 20, 40, or 80 μM) for 24, 48, 72, or 96 h. Following the incubation period, 10 μl of CCK-8 solution was added to each well, and the plates were incubated in a humidified environment with 5% CO_2 at 37 °C. After a 2-h incubation, the optical density (OD) values were measured at 450 nm using a microplate reader (Bio-Tek Instruments, USA). Furthermore, the cytotoxic effects of Ber on bone marrow macrophages (BMMs) were evaluated employing the same CCK-8 assay methodology. To ensure the reliability and reproducibility of the results, all experiments were conducted in triplicate.

High-density culture and toluidine blue staining

To accurately assess the ECM levels in mouse cartilage, we implemented a precise experimental protocol as follows. Initially, approximately 12×10^6 primary chondrocytes were enzymatically dissociated and resuspended in trypsin. Subsequently, 10 μl of the cell suspension was seeded into each well and allowed to adhere at 37 °C for approximately 1 h to facilitate cellular attachment to the substrate. Next, 500 ml of DMEM supplemented with 10% fetal bovine serum (FBS) was added to each well, and the plates were incubated at 37 °C for 24 h. Concurrently, during the incubation phase, interleukin-1 beta (IL-1β) and varying concentrations of Ber (0, 10, and 20 μM) were added to the culture wells. Ultimately, between days 7–9 of the culture period, the cells were fixed with 4% formaldehyde for approximately 30 min and subsequently stained with toluidine blue. The staining intensity was quantified using ImageJ software to determine the ECM levels in the cartilage samples.

RNA extraction and quantitative RT−PCR analysis

In the presence or absence of Ber at concentrations of 10 and 20 μM, 2×105 chondrocytes per well were seeded into 6-well plates and subjected to IL-1β treatment for 48 h. BMMs at a density of 1×10^5 cells per well were seeded into 6-well plates and stimulated with RANKL (50 ng/ml) and M-CSF (30 ng/ml) for 5−7 days. Total RNA was extracted from chondrocytes using TRIzol (Takara Bio, Otsu, Japan) according to the manufacturer's protocol. RNA purity and quality were assessed by measuring the A260/A280 ratio. Subsequently, 1000 ng of total RNA was reverse transcribed into cDNA using reverse transcriptase (Takara Bio, Otsu, Japan) according to the manufacturer's instructions. Real-time PCR was conducted using the LightCycler®480 system (Roche, Germany) and FastStart Universal SYBR Green Master Mix (Roche, Germany) with the following cycling conditions: initial denaturation at 94 °C for 5 s, followed by extension at 60 °C for 30 s, followed by 40 cycles. The expression levels of the target mRNAs were normalized to the GAPDH levels and compared to those in the control group. The specific primer sequences utilized are detailed below (Table1):

Western blot analysis

Total protein was extracted using RIPA lysis buffer, followed by centrifugation, and the protein concentrations were determined using a BCA protein assay kit following the manufacturer's protocol. Equal amounts of protein (40 ng) were separated by 10% SDS−PAGE and then transferred to PVDF membranes (0.45 μm, Millipore, Bedford, MA, USA). After blocking with 5% skim milk for 1 h at room temperature, the membranes were incubated with specific primary antibodies overnight at 4 °C (details of the primary antibodies used in this study can be seen in the Table 2 below). Subsequently, the cells were washed three times with TBST and incubated with the appropriate secondary antibody (1:500) at room temperature for 2 h. Finally, protein bands on the membrane

Gene	Primer sequence	5′-primer-3′
COL2a1	Forward	CTCAAGTCGCTGAACAACCA
	Reverse	GTCTCCGCTCTTCCACTCTG
SOX9	Forward	GCAGGCGGAGGCAGAGGAG
	Reverse	GGAGGAGGAGTGTGGCGAGTC
ADAMTS5	Forward	GCAGAACATCGACCAACTCTACTC
	Reverse	CCAGCAATGCCCACCGAAC
MMP13	Forward	TGTTTGCAGAGCACTACTTGAA
	Reverse	CAGTCACCTCTAAGCCAAAGAAA
NFATC1	Forward	GAGTACACCTTCCAGCACCTT
	Reverse	TATGATGTCGGGGAAAGAGA
C-FOS	Forward	CCAGTCAAGAGCATCAGCAA
	Reverse	AAGTAGTGCAGCCCGGAGTA
CTSK	Forward	AGCAGAACGGAGGCATTGACTC
	Reverse	CCCTCTGCATTTAGCTGCCTTTG
GAPDH	Forward	CGACTTCAACAGCAACTCCCACTCTTCC
	Reverse	TGGGTGGTCCAGGGTTTCTTACTCCTT

Table 1. Sequences used for quantitative real-time PCR.

Name	Molecular weight	Dilution ratio	Company and catalogue Number
COL2A1	142 kDa	1:400	Boster, (A00517-1)
SOX9	70 kDa	1:500	Boster, (A00177-3)
ADAMTS5	75 kDa	1:500	Abcam, (ab45042)
MMP13	54 kDa	1:3000	Abcam, (ab39012)
Bax	21 kDa	1:1000	Proteintech, (60267-1-Ig)
Bcl2	26 kDa	1:1000	Proteintech, (68103-1-Ig)
Cleaved caspase3	17 kDa	1:500	Wanlei, (WL01992)
Caspase3	32 kDa	1:500	Wanlei, (WL04004)
NFATC1	101 kDa	1:10,000	Abcam, (ab264530)
C-FOS	62 kDa	1:1000	Cell Signaling Technology, (2250)
CTSK	37 kDa	1:1000	Abcam, (ab187647)
p-Stat3	88 kDa	1:1000	Santa Cruz Biotechnology, (sc-293,059)
Stat3	88 kDa	1:1000	Santa Cruz Biotechnology, (sc-8019)
p-p65	65 kDa	1:1000	Cell Signaling Technology, (3039)
P65	65 kDa	1:1000	Cell Signaling Technology, (4764)
IκBα	39 kDa	1:1000	Proteintech, (51066-1-AP)
c-Jun	46 kDa	1;500	Boster, (BM4168)
Actin	42 kDa	1:5000	Proteintech, (20536-1-AP)

Table 2. The Company and Catalogue number of all primary antibodies.

were visualized using an enhanced chemiluminescence (ECL) kit and analysed for quantification using ImageJ software (National Institutes of Health, Bethesda, MD) (Supplementary Information).

Immunofluorescence staining

Chondrocytes were seeded at a density of 3×104 cells per well in 24-well plates and cultured for 48 h. Subsequently, the chondrocytes were fixed for 30 min at room temperature and treated with 0.1% Triton X-100 (Sigma Aldrich, Germany) for 10 min. Next, the cells were blocked with 1% BSA (Sigma Aldrich, Germany) for 30 min, followed by overnight incubation at 4 °C with primary antibodies targeting MMP13 and COL2A1. Finally, the chondrocytes were visualized and imaged using a Leica fluorescence microscope.

TUNEL staining

Apoptotic cells in the cartilage cell population were identified using terminal deoxynucleotidyl transferase dUTP nick end labelling (TUNEL) staining according to the manufacturer's instructions. The number of TUNEL-positive cells was quantified.

Flow cytometry analysis

Chondrocytes were seeded on 6-well plates at a density of 3.0×105 cells per well and exposed to varying concentrations of Ber (0, 10, or 20 μM) for 24 h. Following treatment, the cells were harvested and subjected to staining with Annexin V-PE and 7-AAD using assay kits according to the manufacturer's protocol.

TRAP staining assay

BMMs were cultured in a 96-well plate at a density of 8×10^3 cells/well in Dulbecco's modified Eagle's medium (DMEM) supplemented with 30 ng/mL macrophage colony-stimulating factor (M-CSF), 50 ng/mL receptor activator of nuclear factor kappa-B ligand (RANKL), and varying concentrations of Ber (0, 10 and 20 μM) for 5–7 days. The culture medium was refreshed every three days. Upon the appearance of a substantial population of mature osteoclasts in the control well, these cells were specifically stained utilizing a tartrate-resistant acid phosphatase (TRAP) staining kit. Cells exhibiting TRAP positivity with three or more nuclei were counted, and their respective areas were quantitatively assessed.

F-actin ring formation evaluation

BMMs were cultured on glass coverslips and treated with 50 ng/mL RANKL and Ber at concentrations of 0, 10, and 20 μM. After 5–7 days of cell culture, mature osteoclasts fixed in 4% formaldehyde for 20 min were subjected to permeabilization with 0.1% (v/v) Triton X-100 (Sigma−Aldrich) for 5 min and rinsed three times with phosphate-buffered saline (PBS). Nuclei were stained using 4′,6-diamidino-2-phenylindole (DAPI), while F-actin was visualized with phalloidin-tetramethylrhodamine isothiocyanate. The arrangement of F-actin rings was examined using an LSM5 confocal microscope (Carl Zeiss, Oberkochen, Germany) and analysed with Zeiss ZEN software.

DMM-induced OA mice model

C57BL/6 mice (10 weeks old, male, n = 18) were anaesthetised by intraperitoneal injection of 10% chloral hydrate before knees were prepared for aseptic surgery. The connection between the medial meniscus and the tibial plateau (medial meniscus ligament) of the right knee of the mice was subsequently severed using a microsurgical scalpel. The surgical approach is described as follows[22]: We first dissected the fat pad on the cranial horn of the medial meniscus using Jewelers forceps, then took care to identify and avoid the lateral meniscus ligament (LMTL), which is located posteriorly and has fibres oriented in a similar direction to the lateral meniscus ligament. The medial meniscus ligament is then incised with microsurgical scissors, a microsurgical scalpel, or an 11-gauge blade with the blade facing proximally, thereby destabilising the medial meniscus (DMM). After destabilisation of the medial meniscus, the medial meniscus undergoes a medial shift and weight bearing is concentrated in a smaller area, resulting in increased local mechanical stress. The animals were randomly divided into three groups: non-DMM group, DMM group, and DMM + 25 mg/kg Ber group. In the non-DMM group, only the right knee joint was incised, and the tibiofibular ligament of the medial meniscus was not removed. 25 mg/kg was injected intra-articularly into the joint cavity of the DMM plus 25 mg/kg Ber group twice a week for 8 weeks. The non-DMM and DMM groups received the same dose of PBS. All mice were euthanised and knee tissue samples were collected for further analysis at 8 weeks postoperatively. All animal experiments comply with the ARRIVE guidelines and be carried out in accordance with the U.K. Animals (Scientific Procedures) Act, 1986 and associated guidelines. And we confirmed that all animal experiments were reviewed and approved by the Animal Ethics Committee of the First Affiliated Hospital of Nanchang University (protocol number: CDYFY-IACUC-202310QR044).

Histological assessment

Knee joints of mice in each group were fixed in 4% formaldehyde for 24 h, then decalcified in 10% ethylenediaminetetraacetic acid (EDTA) for four weeks and embedded in paraffin. Five micron thick mouse knee joints in paraffin blocks were cut into different planes and stained with hematoxylin and eosin (H&E) and safranin O-fast green.

Statistical analysis

All the data are expressed as the means ± SDs (standard deviations). Each experiment was conducted independently at least three times. Statistical analyses were performed utilizing Student's t test or analysis of variance (ANOVA) with GraphPad Prism software version 8.0 (GraphPad Software, San Diego, CA, USA). P values less than 0.05 were considered to indicate statistical significance.

Results

Ber and OA

As shown in Fig. 1A, 224 potential Ber targets were screened in the PharmMapper database and BATMAN-TCM online tools, while a total of 2354 OA-related targets were screened in the DisGENET database, GeneCards database, DrugBank, TTD database, and PharmGKB, among which 94 common targets of Ber and OA were found, including caspase3 and MMP13. Moreover, the enrichment and analysis of the GO pathways showed that the common targets were mainly involved in the biological functions of collagen catabolism and extracellular matrix recombination (Fig. 1B). To investigate the proteins that have a major impact on metabolism, we performed a protein−protein interaction (PPI) analysis (Fig. 1C), which showed that MMP9, MMP13, and caspase3 were enriched. MMP9 and MMP13 are matrix metalloproteinases that degrade the extracellular matrix of cartilage cells, causing OA[23,24]. Caspase3 is a well-known key protein for apoptosis, and triggering the apoptosis of chondrocytes further triggers OA[25]. Therefore, the PPI-enriched molecules further validated the results obtained by the GO pathway analysis. In addition, molecular docking was performed to observe the binding ability of Ber and the aforementioned hub genes. As shown in Fig. 1D,E, the affinity of Ber for MMP13 and caspase3 was less than − 6 kcal/mol, indicating a strong binding force. Therefore, this study focused mainly on exploring whether Ber can treat OA through the protective effect of the extraoral matrix, alleviating chondrocyte apoptosis and inhibiting osteoclast differentiation.

Ber has a stabilizing effect on IL-1β-induced ECM homeostasis in vitro

To detect the toxic effect of Ber on chondrocytes, ATDC5 cells were incubated with different concentrations of Ber for different durations. The viability of the cells was assessed by a CCK-8 assay. As shown in Fig. 2A, Ber did not show significant cytotoxicity at concentrations less than 20 μM. This result indicates that different concentrations of Ber, such as 0, 10, or 20 μM, can be used in this study for subsequent in vitro experiments. IL-1β plays a key role in cartilage degradation by not only downregulating the synthesis of the extraoral matrix but also promoting the degradation of the extraoral matrix. To investigate the possible protective effect of Ber on the ECM in vitro, we stimulated ATDC5 cells cultured at high density with IL-1β at 7–9 d/s without or with different Ber concentrations and identified the cartilage matrix via toluidine blue staining. As shown in Fig. 2B,C, toluidine blue staining revealed that the intensity of blue staining in the Il-1β-stimulated group was significantly lower than that in the control group. After treatment with 10 μM Ber and 20 μM Ber, the cell cyanosis intensity increased compared with that in the Il-1β stimulation group ($p < 0.05$), indicating that the cyanosis intensity decreased in a dose-dependent manner with increasing Ber dosage. These results suggest that Ber can stabilize IL-1β-stimulated disturbances in ECM homeostasis.

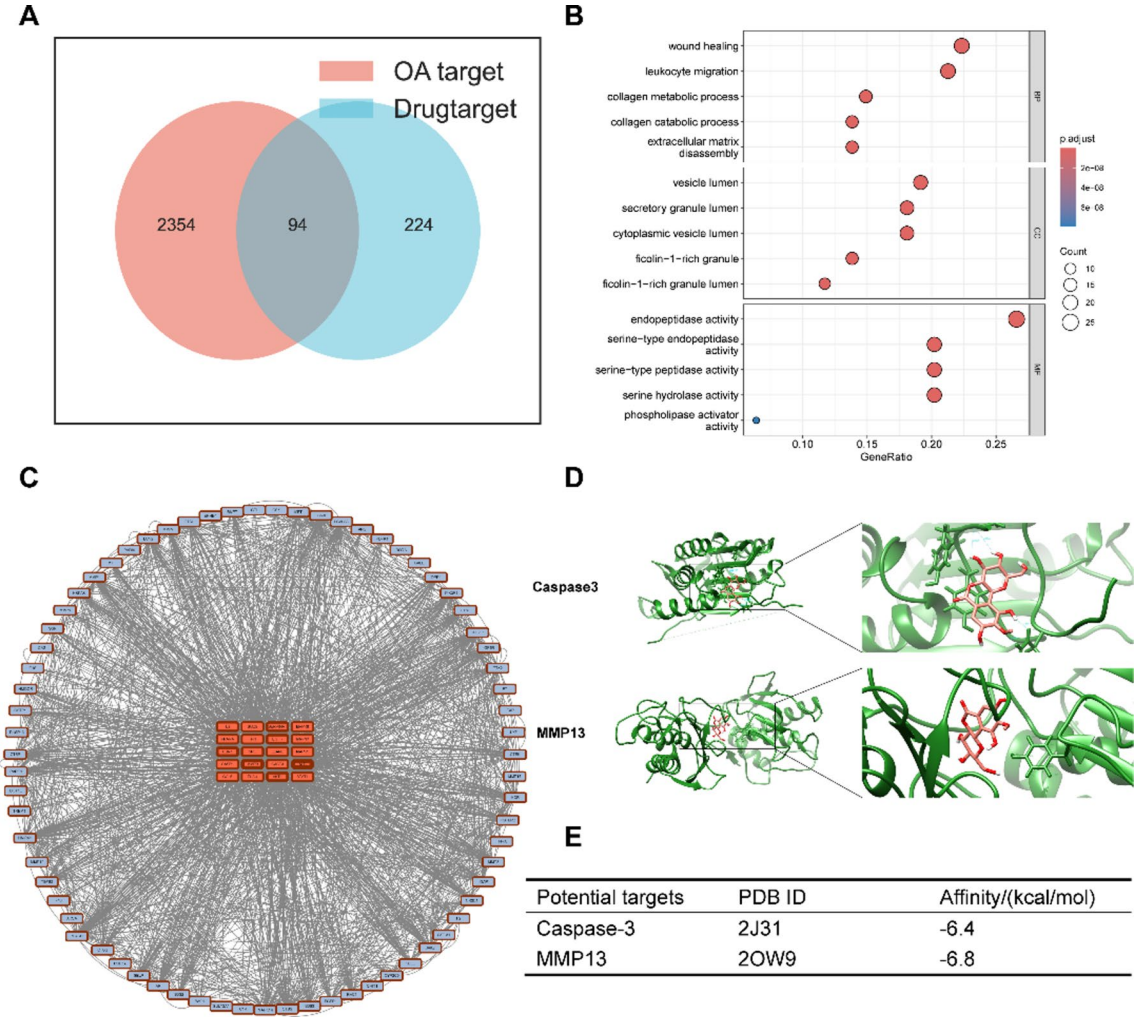

Potential targets	PDB ID	Affinity/(kcal/mol)
Caspase-3	2J31	-6.4
MMP13	2OW9	-6.8

Fig. 1. Network pharmacological analysis. (**A**) Venn diagrams of potential targets of Ber and OA. (**B**) The top 5 items from GO enrichment including Biological process (BP), Cellular component (CC), Molecular function (MF). (**C**) Core targets screening in the PPI network. (**D**) Molecular docking between Ber and Caspase3. Molecular docking between Ber and MMP13. (**E**) The docking energy between Ber and its potential targets. OA, osteoarthritis; Ber, Bergenin.

Ber has a protective effect on IL-1β-induced ECM degradation in chondrocytes

Previous studies have shown that SOX9 is a key gene in chondrocyte differentiation, and it further promotes the expression of COL2A to form type II collagen, which serves as the main architecture of the ECM in chondrocytes[26]. Moreover, ADAMTS5 and MMP13 are the main ECM-degrading enzymes involved in the development of osteoarthritis[27]. To investigate whether Ber has a protective effect on the degradation of the cartilage matrix, we evaluated the expression of SOX9, COL2A1, ADAMTS5, and MMP13 in IL-1β-treated ADTC5 cells, as shown in Fig. 3A–C. Based on the results of real-time quantitative PCR and western blotting, we found that compared with those in the control group, the expression of SOX9 and COL2A1 was significantly downregulated in the IL-1β stimulation group, while the expression of ADAMTS5 and MMP13 was significantly upregulated. However, after Ber administration, the expression of SOX9 and COL2A1 recovered, and the expression of ADAMTS5 and MMP13 tended to normalize in a dose-dependent manner. These results were consistent with the RT−qPCR results. The immunofluorescence staining results of COL2A1 and ADAMTS5 were consistent with those of western blotting and RT−qPCR analysis (Fig. 3D). In summary, the results suggest that Ber has a protective effect on IL-1β-induced ECM degradation in chondrocytes.

Ber alleviated chondrocyte apoptosis induced by Il-1β

Articular cartilage completely depends on the secretion of extracellular matrix by chondrocytes to maintain the homeostasis of its microenvironment. Therefore, the apoptosis of chondrocytes seriously damages articular cartilage and subsequently leads to the occurrence of osteoarthritis[25]. Shi et al. showed that the inflammatory factor IL-1β induced the apoptosis of chondrocytes through ER stress (ERS)[28]. To explore the underlying mechanisms of Ber, KEGG analysis was performed. As shown in Fig. 4A, both the apoptosis and osteoclast differentiation pathways were enriched. To further confirm the effect of Ber on chondrocyte apoptosis, we conducted a follow-up

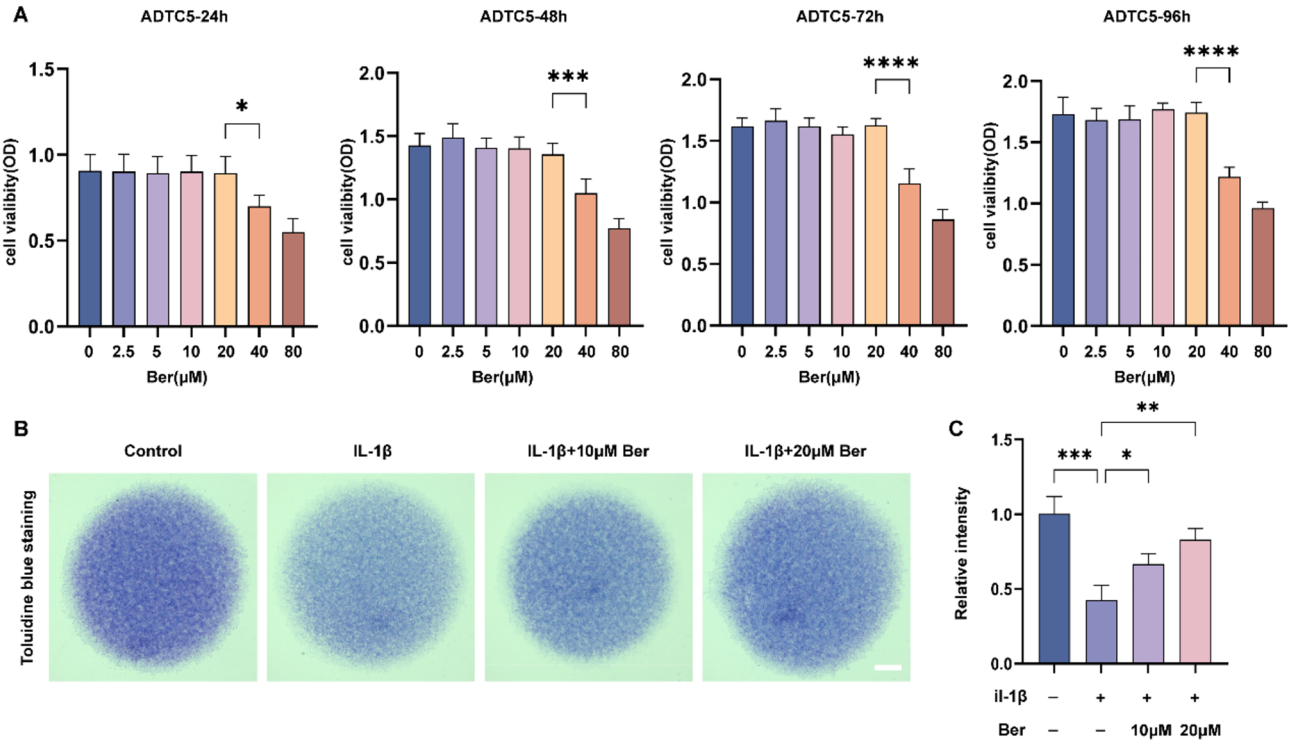

Fig. 2. Bergenin stabilized the disorders of ECM homeostasis stimulated by IL-1β in vitro. (**A**) The cytotoxic effect of Ber on chondrocytes was determined at different concentrations (0, 2.5, 5, 10, 20, 40 and 80 μM) for 24 h, 48 h, 72 h and 96 h. The viability of cells was assessed by CCK-8 assay. (**B**) Toluidine blue staining results for ATDC5 cultured with IL-1β (10 ng/ml) and various concentrations of Ber (0, 10 and 20 μM) for 7–9 days by high density culture method. Scale bar = 1 cm. (**C**) The relative intensity of blue staining. Each column represents the mean ± SD from 3 repeated and independent experiments. *P < 0.05, **P < 0.01, ***P < 0.001 and ****P < 0.0001. ECM, extracellular matrix; IL-1β, interleukin-1β.

experiment based on KEGG data analysis. The western blotting results are shown in Fig. 4B,E. Compared with that in the control group, the expression of the key proapoptotic protein Bax/Bcl-2 in the IL-1β-stimulated group was increased, while the cleaved caspase3/caspase3 ratio was significantly increased. Compared with those in the IL-1β-stimulated group, the ratios of Bax/Bcl-2 and cleaved caspase3/caspase3 in the IL-1β-stimulated group decreased in a dose-dependent manner, and the ratios tended to normalize. TUNEL staining (Fig. 4C,F) also showed that Ber administration had a dose-dependent protective effect on IL-1β-induced chondrocyte apoptosis. Flow cytometry (Fig. 4D,G) showed that IL-1β significantly induced chondrocyte apoptosis, which could be effectively prevented by treatment with different concentrations of Ber. Combining the above results and analysis, Ber inhibited IL-1β-induced chondrocyte apoptosis, which was achieved through downregulation of Bax/Bcl-2 and cleaved caspase3/caspase3 expression.

Ber inhibited RANKL-induced osteoclast differentiation

Many studies have confirmed that blocking the RANKL/RANK interaction can significantly inhibit osteoclast formation. To investigate the toxic effect of Ber on BMMs, we used a CCK-8 assay to assess the viability of BMMs incubated with different concentrations of Ber for different durations (Fig. 5A). This result indicates that different concentrations of Ber, such as 0, 10, or 20 μM, can be used for subsequent experiments to study the mechanism by which Ber inhibits osteoclast differentiation in vitro. We used RT−PCR (Fig. 5B) and western blotting (Fig. 5C,D) to detect the mRNA expression of osteoclast marker genes (NFATC1, C-FOS, CTSK) and found that Ber reversed the upregulated expression of osteoclast marker genes induced by RANKL/RANK. The F-actin loop plays a key role in osteoclast-driven bone resorption. Therefore, we also investigated the effect of Ber on Factin loop production within BMMs during RANKL-induced osteoclastogenesis. We quantified the Factin loop using immunofluorescence assays. The results showed that the F-actin ring was significantly polarized during RANKL-induced osteoclastogenesis, while Ber reduced the number and area of F-actin rings in a dose-dependent manner (Fig. 5E,G). TRAP staining revealed a gradual decrease in the number and size of mature multinucleated osteoclasts with increasing concentrations of Ber (Fig. 5E,F).

Ber inhibited the activation of the NF-κB and STAT3 pathways in IL-1β-treated chondrocytes

To further explore the underlying mechanisms of the effects of Ber on OA, Metascape was used to predict the top 20 pathways of the cotargets. The results indicated that Ber regulates the Jun, NF-κB and STAT3 pathways, which are ranked 1st, 3rd and 5th, respectively (Fig. 6A). Therefore, we conducted further in vitro experiments to investigate whether these signalling pathways are involved in the chondrocyte inflammatory response using

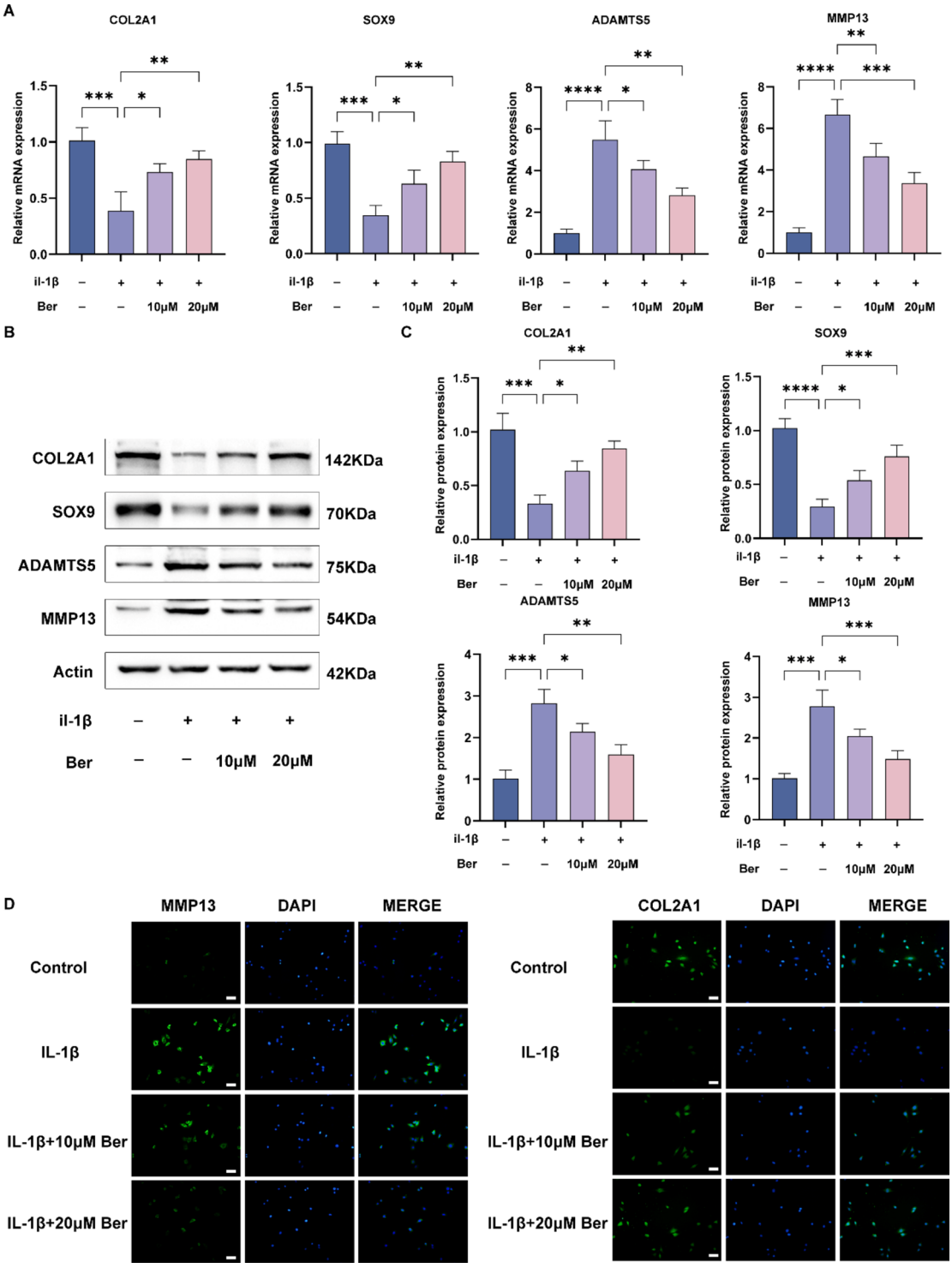

Fig. 3. Bergenin promoted cartilage matrix synthesis and inhibited IL-1β-induced extracellular matrix degradation in ATDC5 cells. (**A**) RT-qPCR was used to evaluate the expression levels of genes related to extracellular matrix synthesis and catabolism, including COL2A1, SOX9, ADAMTS5, MMP13. (**B**) Western blotting was used to detect the expression levels of extracellular matrix anabolic- and catabolic-related proteins (COL2A1, SOX9, ADAMTS5, MMP13) in ATDC5 cells. (**C**) Statistical analysis of protein gray value in (**B**). (**D**) MMP13 and COL2A1 were assessed by immunofluorescence staining combined with DAPI staining. Scale bar = 200 μm. The values are mean ± SD for 3 separate experiments. *P < 0.05, **P < 0.01, ***P < 0.001 and ****P < 0.0001.

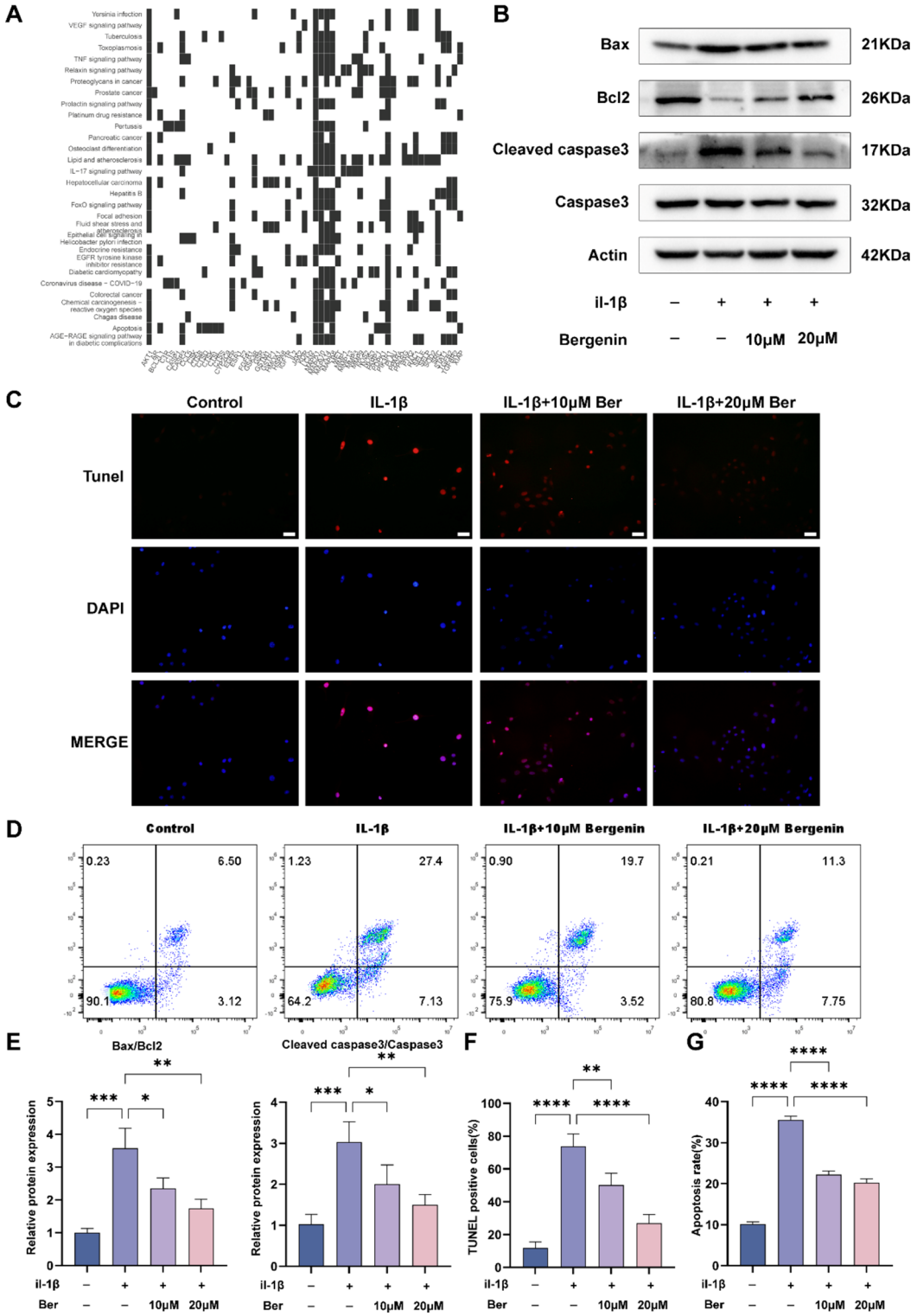

Fig. 4. Effects of Bergenin on IL-1β-induced chondrocyte apoptosis and expression of related genes. (**A**) Diagram of KEGG pathway enrichment. (**B**) Apoptosis-related proteins (Bax, Bcl-2, Cleaved caspase3, Caspase3) were monitored by western blotting. (**C**) The TUNEL assay was used to assess the anti-apoptosis effect of Ber in IL-1β-induced chondrocytes. Scale bar = 200 μm. (**D**) Apoptosis rates for IL-1β-stimulated chondrocytes were analyzed by flow cytometry with annexin V-FITC/PI apoptosis analysis. (**E**) The density of the western blot bands in (**B**) were quantified by ImageJ. (**F**) TUNEL positive cells were quantified in (**C**). (**G**) The data indicated the percentages of apoptotic cells, which were statistically analysis and detected by flow cytometry in (**D**). The values are mean ± SD for 3 separate experiments. *P < 0.05, **P < 0.01, ***P < 0.001 and ****P < 0.0001.

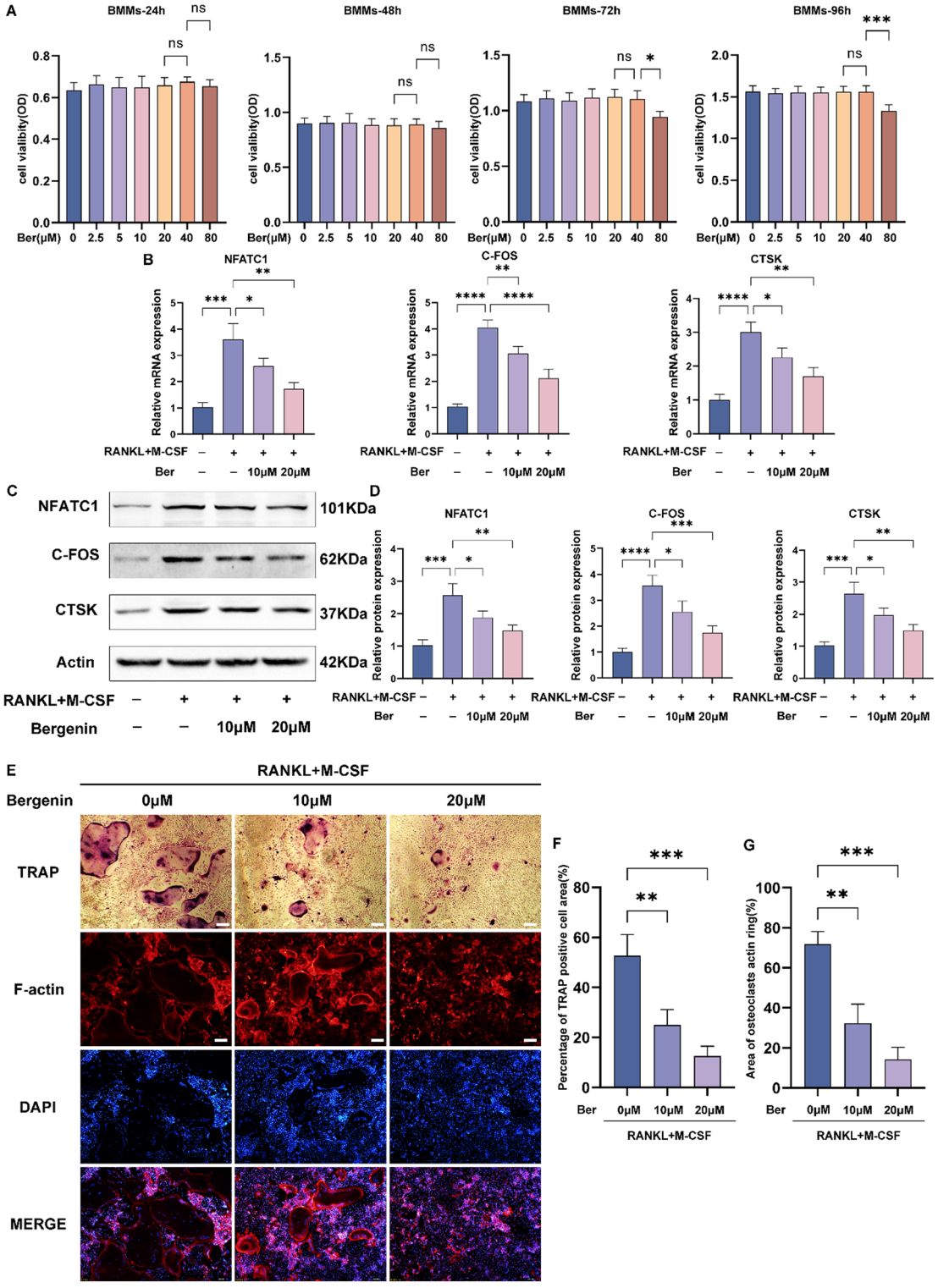

Fig. 5. Bergenin inhibits RANKL-induced osteoclast differentiation in vitro. (**A**) Cytotoxic effects of Ber in BMMs after treatment for 24 h, 48 h, 72 h and 96 h. (**B**) mRNA expression of osteoclast marker genes (NFATC1, C-FOS and CTSK) were detected by RT-qpcr. (**C**) Western blotting performed that Ber suppressed the activation of osteoclast related protein (NFATC1, C-FOS and CTSK). (**D**) The density of the western blot bands in (**C**) were quantified by ImageJ. (**E**) F-actin ring and TRAP staining results for BMMs cultured with M-CSF (30 ng/ml), RANKL (50 ng/ml), and different concentrations of Ber (0, 10 and 20 μM) for 5–7 days. (**F**) The TRAP-positive area of osteoclasts was quantified per well. (**G**) The area of osteoclasts F-actin ring was quantified. The values are mean ± SD for 3 separate experiments. *P < 0.05, **P < 0.01, ***P < 0.001 and ****P < 0.0001.

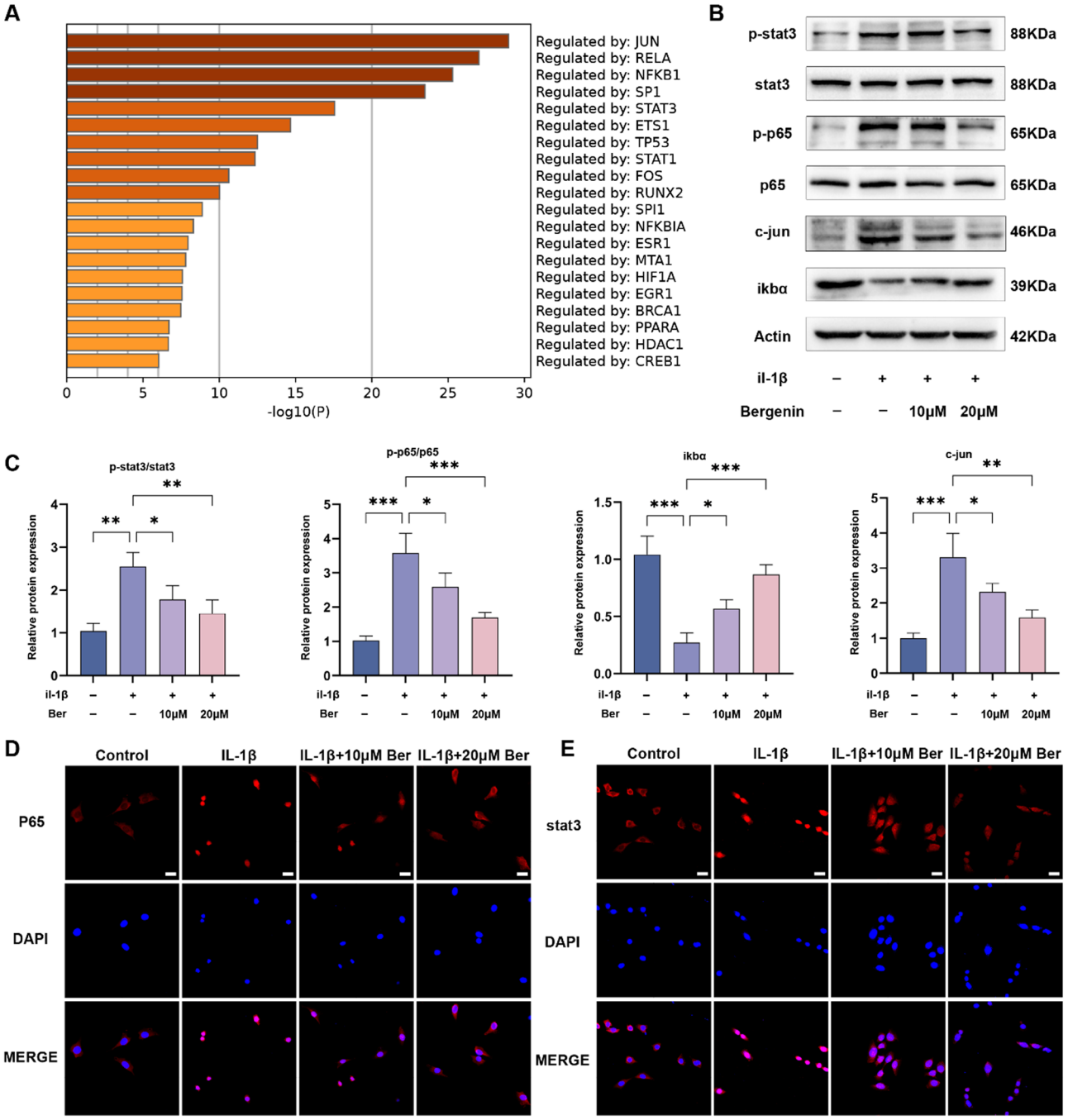

Fig. 6. Effects of Bergenin on NF-κB and STAT3 pathways in IL-1β-treated chondrocytes. (**A**) The top 20 pathways of co-targets. (**B**) Western blotting performed the activity of NF-κB, STAT3 and Jun signaling pathways in chondrocytes. (**C**) ImageJ software was used to quantify the density of western blotting bands shown in (**B**). (**D**) Immunofluorescence staining was used to determine nuclear translocation of p65 in chondrocytes. (**E**) The nuclear translocation of STAT3 was measured by immunofluorescence staining. Scale bar = 100 μm. The values are mean ± SD for 3 separate experiments. *P < 0.05, **P < 0.01, ***P < 0.001 and ****P < 0.0001.

Western blotting and cellular immunofluorescence techniques. As the western blotting results demonstrated, Ber inhibited the expression of c-Jun and the phosphorylation of STAT3 and p65 in parallel with promoting the expression of IκBα in IL-1β-treated chondrocytes (Fig. 6B,C). Moreover, similar results were detected by cellular immunofluorescence, which revealed that Ber attenuated the nuclear translocation of p65 and STAT3 (Fig. 6D,E). All of the above findings indicate that Ber suppressed the activation of the Jun, NF-κB and STAT3 pathways in chondrocytes treated with IL-1β.

Ber alleviated the progression of OA in DMM-induced OA mice model

We then established DMM-induced OA mouse model to explore the effect of Ber on OA in vivo. By employing HE staining and Safranin O-fast green staining on samples of knee joints in mice, we got the results of H&E staining and Safranin O-fast green staining which show that proteoglycan loss and cartilage erosion were more severe in the DMM group than those in the sham group. However, in Ber treated group the result demonstrated that Ber significantly protect knee joints from proteoglycan loss and cartilage destruction compared with the DMM group (Fig. 7A,B).

Discussion

Osteoarthritis has a complex pathogenesis involving inflammation, immunity, and central nervous system dysfunction and leads to joint damage, damage progression, pain, and disability[29]. Studies have shown that during the progression of the osteoarthritic process, biological and physical crosstalk occurs between bone cartilage units, leading to irreversible damage in the osteochondral units[30]. Therefore, only interventions in the early stages of OA can save the osteochondral units from considerable structural and functional changes. In this study, the experiment in vivo show that Ber has a therapeutic effect on OA by reducing proteoglycan loss and cartilage erosion (Fig. 7). However, the mechanism of action is not clear. we used network pharmacological analysis to uncover potential mechanisms for the treatment of OA by Ber. The results revealed therapeutic mechanisms associated with collagen catabolism and extracellular matrix recombination, as well as the apoptosis-associated molecule Caspase3 and the matrix metalloproteinase MMP13 (Fig. 1), the experiment in vivo suggest that Ber has articular cartilage is composed mainly of chondrocytes, type II collagen aggrecan, and 70% water[31]. IL-1β is involved in the development of OA by inducing chondrocytes to release MMPs and thromboxane-based catabolic enzymes, as well as ADATMS4, 5, which leads to the degradation of COL2A1 and aggrecan in the cartilage matrix, inducing cartilage matrix catabolism[32]. The network pharmacology results suggested that the therapeutic mechanism may be related to collagen catabolism and extracellular matrix recombination, therefore we investigated these predicted mechanisms in ADTC5 cells treated with IL-1β. Ber stabilized ECM homeostasis in IL-1β-treated ADTC5 cells (Fig. 2) and upregulated the mRNA and protein expression of COL2A1 and SOX9, which inhibited the mRNA and protein expression of ADATMS5 and SOX9, promoted cartilage matrix synthesis, and inhibited IL-1β-induced ECM degradation in ATDC5 cells (Fig. 3). Based on the network pharmacological results, we further examined the effect of Ber on IL-1β-induced apoptosis in chondrocytes (Fig. 4). The western blotting results showed that Ber alleviated the cell apoptosis caused by IL-1β by downregulating the ratio of Bax/Bcl-2 and cleaved caspase3/caspase3 protein expression. The TUNEL assay combined with flow cytometry reinforced this conclusion. Subchondral bone remodelling plays an important role in the early stages of OA progression, where osteoclasts take up growth factors released from the bone matrix to regulate chondrocyte metabolism and participate in cartilage degradation, and OA chondrocytes also produce a variety of proinflammatory cytokines to promote subchondral bone loss[16,17]. Our results showed that Ber dose-dependently inhibited RANKL-induced osteoclastogenesis and suppressed the mRNA and protein expression of osteoclast-related genes (NFATC1,

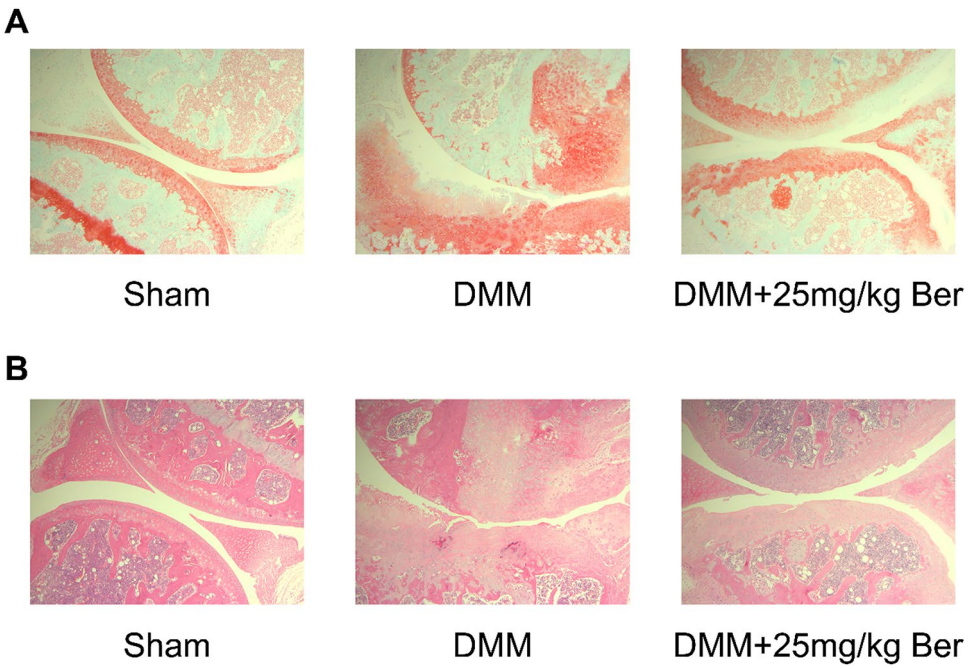

Fig. 7. Ber ameliorates the progression of OA in the DMM model. (**A**) Typical H&E staining of cartilage from different experimental groups. (sham, DMM, and DMM + 25 mg/kg Ber groups). (**B**) Safranin O-Fast Green (S–O) staining of cartilage from different experimental groups (sham, DMM, and DMM + 25 mg/kg Ber groups). Pictures with a magnification of 50 under the microscope. Each group have 6 mice.

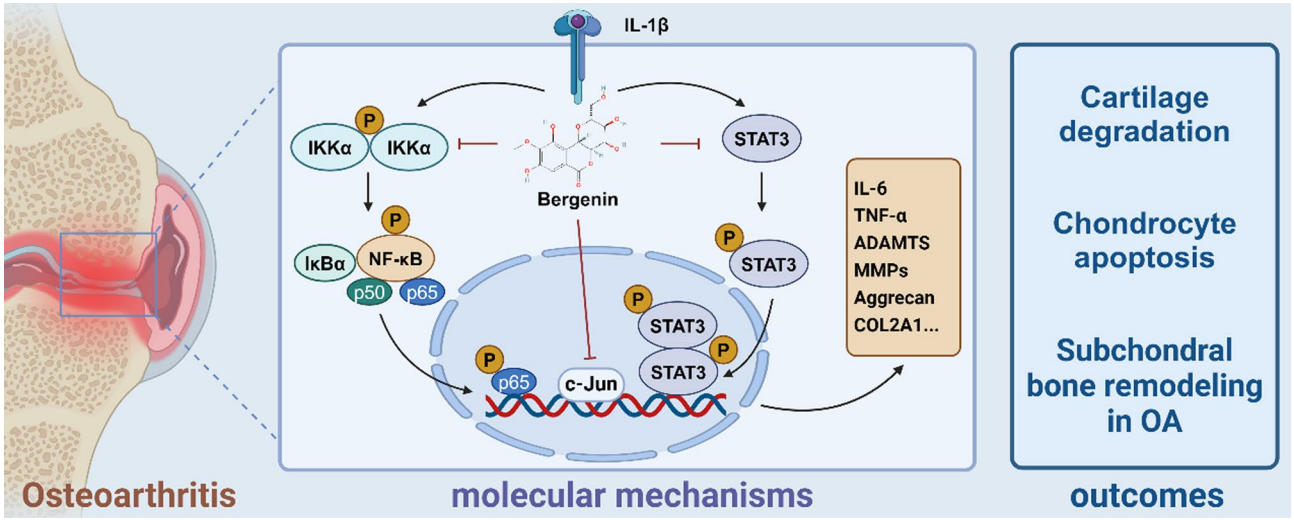

Fig. 8. Schematic of Ber inhibition of inflammatory pathways in ATDC5 cells in vitro. In general, it inhibits the IL-1β-activated NF-κB, STAT3 signaling pathway as well as subsequent phosphorylation upregulation and phosphorylation into the nucleus and Jun signaling pathway. It ameliorates OA by inhibiting the upregulation of inflammatory factors such as MMPs and ADAMTS and protecting COL2A1 and aggrecan from degradation. Finally, above mechanisms contribute to three outcomes including cartilage degradation, chondrocyte apoptosis and subchondral bone remodeling in OA. Created using biorender.com.

C-FOS, and CTSK) in vitro (Fig. 5A–C). In addition, Ber inhibited F-actin ring formation and bone resorption in a dose-dependent manner, demonstrating that Ber antagonized bone loss (Fig. 5D–G).

Jun is a transcription factor that recognises and binds to the AP-1 consensus motif 5′-TGA[GC]TCA-3′[33,34] and heterodimerises with proteins of the FOS family to form the AP-1 transcription complex. Previous studies showed that the increasing expression of Jun leaded to the overexpression of MMPs, contributing the progression of OA[9,10]. The NF-κB signalling pathway regulates the expression of multiple inflammatory mediators and matrix-degrading enzymes and is considered to be an important pathway in the pathological process of OA[35]. IL-1β stimulation of chondrocytes activates IκB kinase, which then leads to IκBα degradation[36]. Subsequent translocation of p65 to the nucleus and its subsequent phosphorylation promote the expression of inflammatory factors (INOS, COX2, IL-6, and TNF-α)[37], contributing to the worsening of OA. Previous studies have shown that the JAK2/STAT3 signalling pathway is aberrantly activated in OA chondrocytes, leading to an imbalance in cartilage homeostasis[38] and that inhibition of this pathway promotes chondrocyte proliferation[39]. In addition, during the progression of OA, chondrocytes release large amounts of inflammatory factors such as IL-1β, which rapidly stimulate STAT3 to undergo phosphorylation and accelerate cartilage degradation. The above studies suggest that STAT3 is important in the development of OA. Through multitarget molecular docking analysis, it has been found that Ber can bind strongly to ALOX15, iNOS, ERBB2, SELE, and NF-κB, and in addition, Ber may regulate inflammatory responses mainly through the NF-κB signalling pathway[40]. Ber can inhibit the phosphorylation of STAT3 and therefore has anticancer activity in cervical cancer[41]. Consistent with our results, Ber inhibited the Jun, NF-κB and STAT3 pathways by suppressing c-Jun, IκBα and the phosphorylation of P65 and STAT3 in IL-1β-treated chondrocytes (Fig. 6).

These results strengthened the credibility of the network pharmacology and confirmed that Ber is a promising agent for treating OA. However, there are several limitations in our study. First, the potential mechanisms by which Ber treats osteoarthritis were proven by network pharmacology combined with experiments. However, we selected only a few network pharmacology results for validation experiments, which may ignore other essential pathways. Additionally, we only conduct a few experiment in vivo, which will be the focus of our follow-up study. More research is necessary to determine whether Ber affects other targets that can delay OA progression.

Conclusion

In summary, our study is the first to employ network pharmacology to predict the potential mechanisms by which Ber affects OA, followed by in vitro and vivo experiments to verify that Ber can alleviate cartilage degradation, chondrocyte apoptosis, and subchondral bone remodelling in OA by inhibiting the Jun, NF-κB and STAT3 signalling pathways (Fig. 8). Taken together, our results suggest that Ber may be an effective drug for the treatment of early OA .

Data availability

The datasets used and/or analysed during the current study are available from the corresponding author upon reasonable request.

Received: 25 May 2024; Accepted: 26 August 2024
Published online: 31 August 2024

References

1. Chen, D. et al. Osteoarthritis: Toward a comprehensive understanding of pathological mechanism. *Bone Res.* **5**, 16044 (2017).
2. Primorac, D. et al. Knee osteoarthritis: A review of pathogenesis and state-of-the-art non-operative therapeutic considerations. *Genes.* **11**(8), 854 (2020).
3. Hawker, G. A. Osteoarthritis is a serious disease. *Clin. Exp. Rheumatol.* **37**(Suppl 120), 3–6 (2019).
4. Wallace, I. J. et al. Knee osteoarthritis has doubled in prevalence since the mid-20th century. *Proc. Natl. Acad. Sci. USA* **114**(35), 9332–9336 (2017).
5. Liu, J. et al. Ghrelin prevents articular cartilage matrix destruction in human chondrocytes. *Biomed. Pharmacother.* **98**, 651–655 (2018).
6. Grandi, F. C. & Bhutani, N. Epigenetic therapies for osteoarthritis. *Trends Pharmacol. Sci.* **41**(8), 557–569 (2020).
7. Cai, Z. et al. Magnoflorine with hyaluronic acid gel promotes subchondral bone regeneration and attenuates cartilage degeneration in early osteoarthritis. *Bone* **116**, 266–278 (2018).
8. Yang, C. Y., Chanalaris, A. & Troeberg, L. ADAMTS and ADAM metalloproteinases in osteoarthritis—looking beyond the "usual suspects". *Osteoarthr. Cartil.* **25**(7), 1000–1009 (2017).
9. Chiu, Y. C. et al. Stromal cell-derived factor-1 induces matrix metalloprotease-13 expression in human chondrocytes. *Mol. Pharmacol.* **72**(3), 695–703 (2007).
10. Nishitani, K. et al. PGE2 inhibits MMP expression by suppressing MKK4-JNK MAP kinase-c-JUN pathway via EP4 in human articular chondrocytes. *J. Cell Biochem.* **109**(2), 425–433 (2010).
11. Urban, H. & Little, C. B. The role of fat and inflammation in the pathogenesis and management of osteoarthritis. *Rheumatology* **57**(suppl_4), iv10–iv21 (2018).
12. Robinson, W. H. et al. Low-grade inflammation as a key mediator of the pathogenesis of osteoarthritis. *Nat. Rev. Rheumatol.* **12**(10), 580–592 (2016).
13. Lepetsos, P., Papavassiliou, K. A. & Papavassiliou, A. G. Redox and NF-κB signaling in osteoarthritis. *Free Radic. Biol. Med.* **132**, 90–100 (2019).
14. Li, G. et al. Identical subchondral bone microarchitecture pattern with increased bone resorption in rheumatoid arthritis as compared to osteoarthritis. *Osteoarthr. Cartil.* **22**(12), 2083–2092 (2014).
15. Cao, Y. et al. IL-1β differently stimulates proliferation and multinucleation of distinct mouse bone marrow osteoclast precursor subsets. *J. Leukoc. Biol.* **100**(3), 513–523 (2016).
16. Li, Z., Huang, Z. & Bai, L. Cell interplay in osteoarthritis. *Front. Cell Dev. Biol.* **9**, 720477 (2021).
17. Hu, W., Chen, Y., Dou, C. & Dong, S. Microenvironment in subchondral bone: Predominant regulator for the treatment of osteoarthritis. *Ann. Rheum. Dis.* **80**(4), 413–422 (2021).
18. Salimo, Z. M. et al. Chemistry and pharmacology of bergenin or its derivatives: A promising molecule. *Biomolecules.* **13**(3), 403 (2023).
19. Jain, S. K. et al. Pyrano-isochromanones as IL-6 inhibitors: Synthesis, in vitro and in vivo antiarthritic activity. *J. Med. Chem.* **57**(16), 7085–7097 (2014).
20. Singh, R., Kumar, V., Bharate, S. S. & Vishwakarma, R. A. Synthesis, pH dependent, plasma and enzymatic stability of bergenin prodrugs for potential use against rheumatoid arthritis. *Bioorg. Med. Chem.* **25**(20), 5513–5521 (2017).
21. Liu, Y., An, Z. & He, Y. The traditional uses, phytochemistry, pharmacology and toxicology of *Bergenia purparescens*: A review comments and suggestions. *Heliyon.* **9**(11), e22249 (2023).
22. Glasson, S. S., Blanchet, T. J. & Morris, E. A. The surgical destabilization of the medial meniscus (DMM) model of osteoarthritis in the 129/SvEv mouse. *Osteoarthr. Cartil.* **15**(9), 1061–1069 (2007).
23. Li, S. et al. COL3A1 and MMP9 serve as potential diagnostic biomarkers of osteoarthritis and are associated with immune cell infiltration. *Front. Genet.* **12**, 721258 (2021).
24. Hu, Q. & Ecker, M. Overview of MMP-13 as a promising target for the treatment of osteoarthritis. *Int. J. Mol. Sci.* **22**(4), 1742 (2021).
25. Hwang, H. S. & Kim, H. A. Chondrocyte apoptosis in the pathogenesis of osteoarthritis. *Int. J. Mol. Sci.* **16**(11), 26035–26054 (2015).
26. Hardingham, T. E., Oldershaw, R. A. & Tew, S. R. Cartilage, SOX9 and Notch signals in chondrogenesis. *J. Anat.* **209**(4), 469–480 (2006).
27. Wu, Y. et al. Sinomenine contributes to the inhibition of the inflammatory response and the improvement of osteoarthritis in mouse-cartilage cells by acting on the Nrf2/HO-1 and NF-κB signaling pathways. *Int. Immunopharmacol.* **75**, 105715 (2019).
28. Shi, D. et al. IL-1beta induced endoplasmic reticulum stress increases the apoptosis of human chondrocyte. *Basic Clin. Med.* **35**(8), 1089–1093 (2015).
29. Dobson, G. P. et al. Defining the osteoarthritis patient: Back to the future. *Osteoarthr. Cartil.* **26**(8), 1003–1007 (2018).
30. Goldring, S. R. & Goldring, M. B. Changes in the osteochondral unit during osteoarthritis: Structure, function and cartilage-bone crosstalk. *Nat. Rev. Rheumatol.* **12**(11), 632–644 (2016).
31. Armiento, A. R., Stoddart, M. J., Alini, M. & Eglin, D. Biomaterials for articular cartilage tissue engineering: Learning from biology. *Acta Biomater.* **65**, 1–20 (2018).
32. Pujol, J. P. & Loyau, G. Interleukin-1 and osteoarthritis. *Life Sci.* **41**(10), 1187–1198 (1987).
33. Qing, J., Zhang, Y. & Derynck, R. Structural and functional characterization of the transforming growth factor-beta -induced Smad3/c-Jun transcriptional cooperativity. *J. Biol. Chem.* **275**(49), 38802–38812 (2000).
34. Ji, Z. et al. The forkhead transcription factor FOXK2 promotes AP-1-mediated transcriptional regulation. *Mol. Cell Biol.* **32**(2), 385–398 (2012).
35. Marcu, K. B., Otero, M., Olivotto, E., Borzi, R. M. & Goldring, M. B. NF-kappaB signaling: Multiple angles to target OA. *Curr. Drug Targets.* **11**(5), 599–613 (2010).
36. Roman-Blas, J. A. & Jimenez, S. A. NF-kappaB as a potential therapeutic target in osteoarthritis and rheumatoid arthritis. *Osteoarthr. Cartil.* **14**(9), 839–848 (2006).
37. Sun, Y. et al. Poly(ADP-ribose) polymerase 1 inhibition prevents interleukin-1β-induced inflammation in human osteoarthritic chondrocytes. *Acta Biochim. Biophys. Sin.* **47**(6), 422–430 (2015).
38. Ye, X.-M. et al. Epigenetic silencing of miR-375 induces trastuzumab resistance in HER2-positive breast cancer by targeting IGF1R. *BMC Cancer.* **14**(1), 134 (2014).
39. Rong, Y. et al. Hypoxic pretreatment of small extracellular vesicles mediates cartilage repair in osteoarthritis by delivering miR-216a-5p. *Acta Biomater.* **122**, 325–342 (2021).
40. Li, G. et al. Screening and isolation of potential anti-inflammatory compounds from *Saxifraga atrata* via affinity ultrafiltration-HPLC and multi-target molecular docking analyses. *Nutrients.* **14**(12), 2405 (2022).
41. Shi, X. et al. Anticancer activity of bergenin against cervical cancer cells involves apoptosis, cell cycle arrest, inhibition of cell migration and the STAT3 signalling pathway. *Exp. Ther. Med.* **17**(5), 3525–3529 (2019).

Author contributions

Zhiwei Zhang and Bo Li designed, performed most of the experiments and wrote the manuscript. Shuqin Wu performed the network pharmacological analysis and wrote the manuscript. Yuxin Yang and Binkang Wu collected and analyzed the data. Qi Lai, Fuchong Lai, Fengbo Mo and Yufei Zhong helped to revise the manuscript. Song Wang, Runsheng Guo and Bin Zhang guided the experiments. All authors read and approved the final manuscript.

Funding

This study received financial support from the project "protective effect of ADRM1 on osteoarthritis and its mechanism", National Natural Science Foundation of China Regional Project (Grant No. 82160426).

Competing interests

The authors declare no competing interests.

Ethics statement

We confirmed that all animal experiments were reviewed and approved by the Animal Ethics Committee of the First Affiliated Hospital of Nanchang University (protocol number: CDYFY-IACUC-202310QR044). As our study did not involve human beings or human tissues, the patient consent is not applicable.

Additional information

Supplementary Information The online version contains supplementary material available at https://doi.org/10.1038/s41598-024-71259-9.

Correspondence and requests for materials should be addressed to S.W., R.G. or B.Z.

Reprints and permissions information is available at www.nature.com/reprints.

Publisher's note Springer Nature remains neutral with regard to jurisdictional claims in published maps and institutional affiliations.